Draft 12/27/14
Preprint typeset using LaTeX style emulateapj v. 12/16/11

ANGULAR DEPENDENT BISMUTH SELENIDE NMR

Andrea Gaughan[1]

Draft 12/27/14

ABSTRACT

In this paper, I present the results of an angular dependent NMR study on a sample of the material bismuth selenide (Bi_2Se_3) that I synthesized. Bi_2Se_3 has been of much interest in the field of condensed matter physics because of its recent discovery as a topological insulator. The work presented in this paper is a continuation of the work done by David Nisson (Nisson et al. 2014). The NMR studies described in this paper will aid in the characterization of the bulk electronic states of this material, and potentially lay the groundwork for further studies of the conducting surface states.

1. INTRODUCTION

1.1. *Nuclear Magnetic Resonance*

Nuclear magnetic resonance (NMR) allows the experimental probing of the spin states of nuclei through observing the radio frequency transitions between spin energy levels split by a magnetic field. A classical treatment of the precession of a nuclear magnetic moment can be illustrative to one looking to understand the basic concepts of NMR. A magnetic moment in an external magnetic field ($\vec{H}$) experiences torque ($\vec{\tau}$) which is equal to the time derivative of the magnetic moment's angular momentum ($\vec{L}$):

$$\vec{\tau} = \frac{d\vec{L}}{dt} = \vec{\mu} \times \vec{H}$$

The standard equations describing classical precession can be derived from this equation.

$$\begin{aligned} L_x &= L_0 cos(\omega t) \\ L_y &= L_0 sin(\omega t) \\ L_z &= k \end{aligned}$$

where k is a constant and ω is the angular velocity of the magnetic moment.

While the classical treatment of a magnetic moment is helpful for relating aspects of NMR to an intuitive picture, a quantum treatment is necessary to fully describe this quantum phenomenon. Many interactions with nuclei affect the spin states, and these interactions can be denoted neatly in the nuclear spin Hamiltonian:

$$H = H_Z + H_{dip} + H_{hyp} + H_Q,$$

where H_Z is the Zeeman interaction, the interaction of nuclei with the external magnetic field; H_{dip} is the dipole interaction, the interaction with surrounding nuclei; H_{hyp} is the hyperfine interaction, the interaction with the spins of surrounding electrons; and H_Q is the quadrupole interaction, the interaction with the local electric field gradient.

The Zeeman interaction (H_Z) is the interaction of the nucleus with an external magnetic field. In our experiments, this is the largest component of the nuclear spin Hamiltonian. In the absence of an external magnetic field, the energy levels of a spin-1/2 nucleus are degenerate, but when a magnetic field is applied, energy level splitting occurs. This splitting is demonstrated in Figure 1. When only the Zeeman interaction is considered, the spacing between split energy levels is equal. The spacing between these energy levels corresponds to a resonant frequency that would excite the transition. In NMR, exciting the transitions between energy levels is used as a method of examining a nuclei's energy levels.

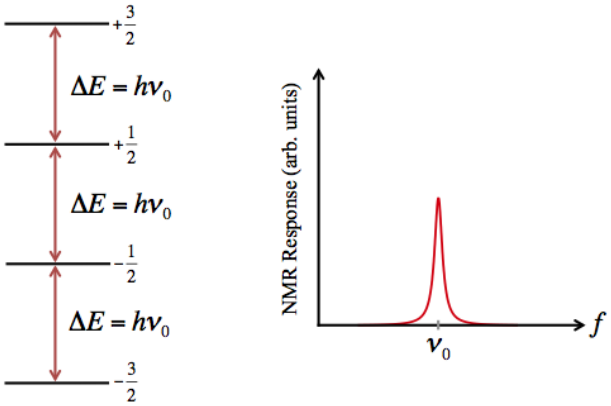

FIG. 1.— Energy level spacing and resulting resonance peak for the example of a nucleus with spin-3/2 due to the Zeeman Interaction. Image from Dioguardi 2013.

The quadrupolar interaction (H_Q) affects a nucleus with spin greater than 1/2. These nuclei can be thought of having an oblong shape, which causes a preferential alignment with the local electric field gradient. This results in different spin states to be unequally split, and each transition has a different resonant frequency, as shown in Figure 2. For nuclei with spin greater than 1/2, the combination of the Zeeman interaction and the quadrupole interaction create a resonant spectrum with as many peaks as there are allowed transitions.

The dipole interaction (H_{dip}) is the interaction between nuclei, which contributes to the line widths of these resonance peaks. The hyperfine interaction (H_{hyp}) is the interaction of a nucleus with surrounding electrons. This interaction causes a shift of all the resonances, which has two components called the often T dependent Knight Shift and the not T dependent chemical shift.

1.2. *Pulsed NMR*

[1] Department of Physics, Haverford College, Haverford, PA 19041, USA

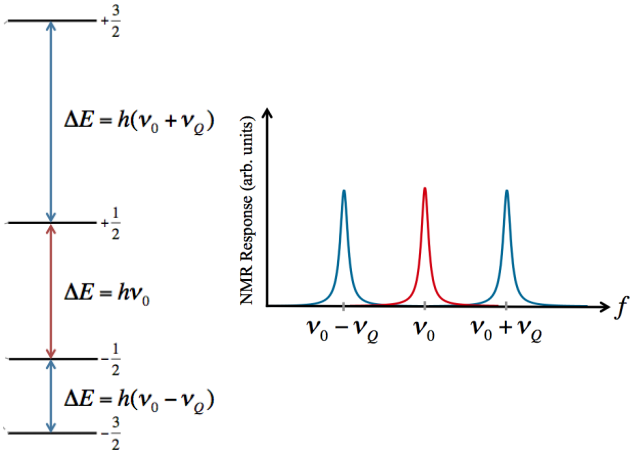

FIG. 2.— Energy level spacing and resulting resonance peaks for the example of a nucleus with spin-3/2 including the effects of the quadrupole interaction and the Zeeman interaction. Image from Dioguardi 2013.

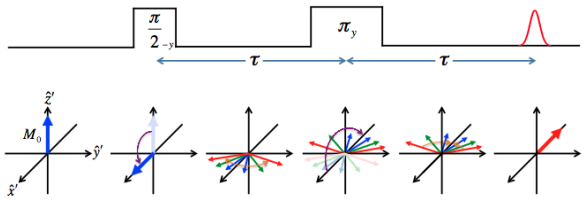

FIG. 3.— Hahn echo pulse sequence and cartoon of resulting effect on nuclei's magnetic moments in the rotating frame. Image from Dioguardi 2013.

Pulsed NMR allows for a specific manipulation of the nuclei's magnetic moments that will maximize the measured response. Our studies use the Hahn echo pulse sequence, which is illustrated in Figure 3.

A initial pulse rotates the magnetic moment 90°, and a second pulse rotates the magnetic moment another 180°, creating an spin echo that can be observed experimentally. The spin echo will be maximized when the initial pulse rotates the magnetic moment exactly 90° at a resonant frequency. This pulse length is known as t_{90}. To find this value, we take measurements called nutations, where we vary the pulse length and find the length with maximum response. Then, through frequency sweeps, we identify the resonant frequency or frequencies.

1.3. *Topological Insulators*

Topological insulators are a novel form of condensed matter that has been extensively studied (Hasan and Kane 2010). A topological insulator is a material that has conducting surface states, while the bulk of the material remains insulating. These materials have potential applications in spintronics, technology that makes use of electron spin states. Spintronics would help overcome the issue of overheating in current electronics, and would allow for technology to built at yet smaller scales than currently possible. Researching the nuclear spin states of the bulk states of topological insulators through NMR, as done in this paper, aids in characterizing the material for potential use.

1.4. *Bismuth Selenide*

Bismuth selenide (Bi_2Se_3) is a topological insulator that has been extensively studied. However, few NMR studies have been done on the material (Taylor et al. 2012; Young et al. 2012; Nisson et al. 2014). NMR is a promising method of studying Bi_2Se_3, as both the elements composing this material have NMR active isotopes. ^{209}Bi is a NMR active isotope of bismuth with 100% natural abundance. ^{209}Bi is spin-9/2, meaning that the quadrupolar interaction will play an important role in the nuclear spin Hamiltonian describing its energy states. Selenium also has an NMR active isotope, ^{77}Se, but this isotope is only 7.5% abundant, meaning that the signal will be more difficult to observe. ^{77}Se is spin-1/2, so the quadrupole interaction will have no effect on the selenium NMR signal.

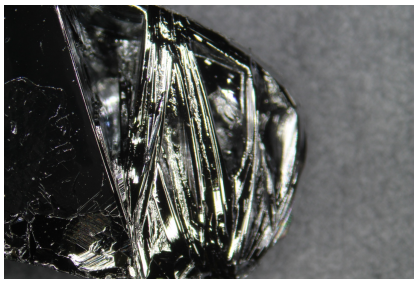

FIG. 4.— Edge of Bi_2Se_3 sample with interesting crystalline structure, with part of smooth crystal surface visible.

2. EXPERIMENTAL METHODS

2.1. *Sample Preperation*

To synthesize Bi_2Se_3, I massed out 1.423g of bismuth and 0.808g of selenium for a total mass of 2.233g and a stoichiometeric ratio of 2:3. The bismuth and selenium were vacuum sealed in a quartz ampoule to avoid any impurities in the sample. The ampoule was heated from 20°C to 800°C at a rate of 20°C/hr, in order to heat the elements well above the melting point of 710°C of Bi_2Se_3. The mixture was held at 800°C for 20 hours to ensure homogeneity of the mixture. Then, the temperature was slowly decreased from 800°C to 500°C at a rate of 6°C/hr to allow a large crystal grain to form. The furnace was allowed to cool, then the sample was extracted from the ampoule. The resulting sample is shown in Figure 4.

We performed x-ray diffraction (XRD) on a powder ground from the edge of the sample in order to confirm the composition of our sample. The XRD data shown in Figure 5 shows that our sample is largely composed of Bi_2Se_3, as desired, with some elemental bismuth left unreacted with selenium. The sample appears to have no other contamination.

We cut a 5x3x0.2mm and 8.5mg crystal of the sample to use for NMR, as shown in Figure 6.

2.2. *Measurement Techniques*

We wrapped a transmitting and receiving coil with 38 AWG wire to fit the cut of our sample. The coil and sample were mounted on our goniometer probe. In all of our studies, the probe was used in our Quantum Design Physical Property Measurement System (PPMS).

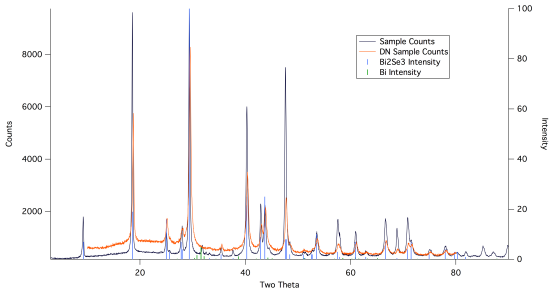

FIG. 5.— X-ray diffraction pattern of Bi_2Se_3 (black) plotted with expected XRD pattern for Bi_2Se_3 (blue), expected XRD pattern for elemental bismuth (green), and the XRD pattern for a pure Bi_2Se_3 sample grown by David Nisson (orange).

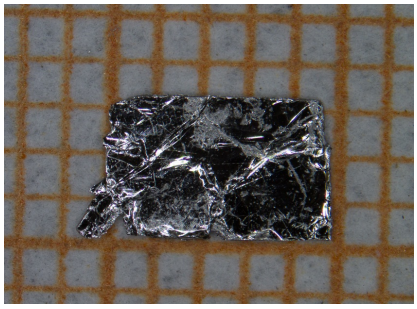

FIG. 6.— Cut of sample for NMR photographed on millimeter graph paper.

All studies were conducted at a constant temperature of 300K and field of 9T.

3. RESULTS AND DISCUSSION

3.1. *Search for ^{77}Se Signal*

From the ^{209}Bi signal in the crystal sample and a known shift from Taylor et al. (2012) we calculated the expected frequency of the ^{77}Se signal. We were unable to detect any signal above the level of noise in the crystal. We ground a powder sample from the original Bi_2Se_3 sample, with a mass of 215mg, approximately 25 times more massive than the cut crystal.

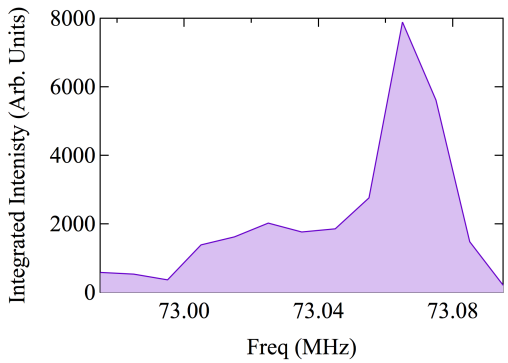

FIG. 7.— Frequency sweep around ^{77}Se signal in the powder sample of Bi_2Se_3. This spectrum closely resembles the theoretical single horn powder pattern.

Although the NMR active isotope of Se is only 7.5% naturally abundant, this larger sample allowed us to find the ^{77}Se signal, as shown in Figure 7. This frequency sweep shows the signature powder pattern. The signal has a characteristic single horn powder pattern because the NMR active isotope of Se is spin-1/2, and thus has only one possible transition between spin states. The powder pattern results from crystal anisotropy and the distribution of crystallite orientations with respect to the external field in a powder.

3.2. *Angular Dependent Study*

We examined the angular dependence of the ^{209}Bi NMR signal in our Bi_2Se_3 crystal cut from the sample for 21 angles ranging from 0° to 90° between the $\hat{c}$-axis and the external magnetic field. At each angle, we took a quick frequency sweep around the central peak to find the central frequency, then nutated at this frequency to find t_{90}. We then took a frequency sweep ranging over the nine resonance peaks of the bismuth signal, using the pulse length of t_{90} found from the nutation.

The nutations and frequency sweeps are shown in Figures 14 and 15. The nutations show drastic changes in t_{90} as a function of angle, with a range from 0.8μs to 5.6μs.

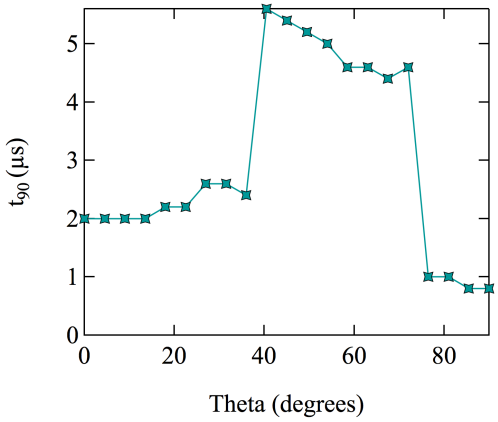

FIG. 8.— t_{90} as a function of angle as determined from the highest intensity peak of each nutation curve.

The evolution of t_{90}, as found from the peak intensity of each nutation, is shown in Figure 8.

In the frequency sweeps, the resonances collapse around 54°, the magic angle - a characteristic angle at which all resonances occur at the same frequency for crystalline structures in a magnetic field. The locations of the peaks, for as long as they are resolvable, is shown in Figure 9. As seen in this figure, in addition to the peaks frequencies shifting towards the central frequency, the central frequency also shifts relatively constantly as a function of angle.

The total signal intensity, found from the area under the frequency spectra, is shown in Figure 10. There is a general decreasing trend, with two dips in signal intensity at 40° and 68°. There is a local maximum at the magic angle.

3.3. *T_2 Study*

In NMR studies, T_2^{-1} is the spin-spin relaxation rate, or transversal relaxation rate. This decay is a result of

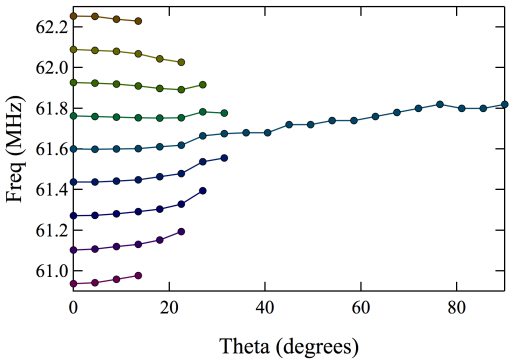

FIG. 9.— Peak frequencies of the ^{209}Bi signal frequency sweeps as a function of angle. Peaks are graphed for all angles they were resolvable.

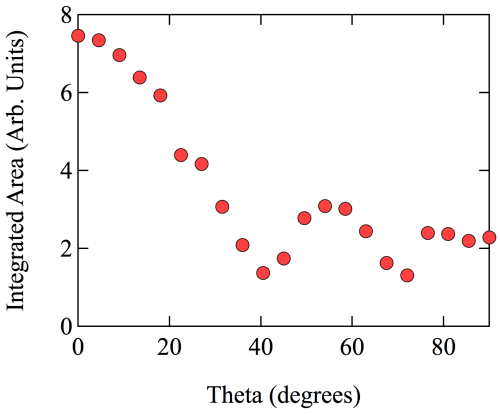

FIG. 10.— Integrated area under ^{209}Bi signal frequency sweeps as a function of angle.

decoherence of the spin echo over time. If T_2^{-1} changes over the spectrum, this would affect the signal intensity at different frequencies.

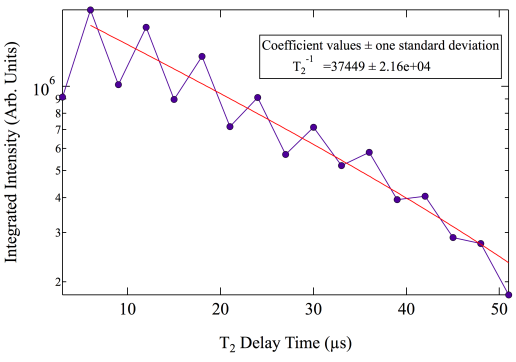

FIG. 11.— T_2 scan at the frequency of the ninth peak at 0°. T_2^{-1} is calculated from a exponential fit.

To investigate the angular dependence of T_2^{-1}, we took a T_2 scan at the frequency corresponding to each of the nine peaks in the 0° spectrum. We maintained a constant difference of 2μs between the parameters off and τ (the T_2^{-1} delay time), as it was in the angular dependent study. Figure 11 shows the T_2 scan for the 9^{th} peak at 62.241MHz. T_2^{-1} was found from an exponential decay fit. The data appears jagged, which we believe is the result of a periodicity of 6μs like that seen in Young et al. (2012). This jaggedness was present in the T_2 scans at all of the peak frequencies. This could be tested by taking these measurements again with closer spacing between data points.

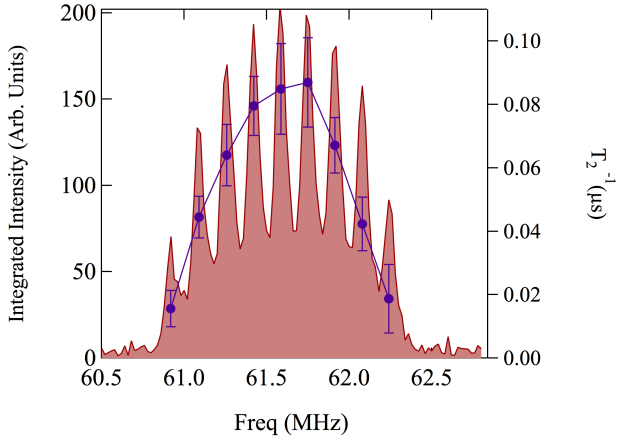

FIG. 12.— Values of T_2^{-1} at each frequency corresponding to the nine peaks of the 0° spectrum plotted over the 0° spectrum.

Figure 12 shows the fitted values for T_2^{-1} from each of the nine measurements plotted over the 0° spectrum. There is evidently a strong frequency dependence on T_2^{-1}. This helps explain the decrease in signal at the satellite peaks. The large error bars on the values of T_2^{-1} are partially a result of the periodic behavior of the T_2 scans. If we took more data in the future, we could combine a periodic and exponentially decaying fit to decrease the error in our values.

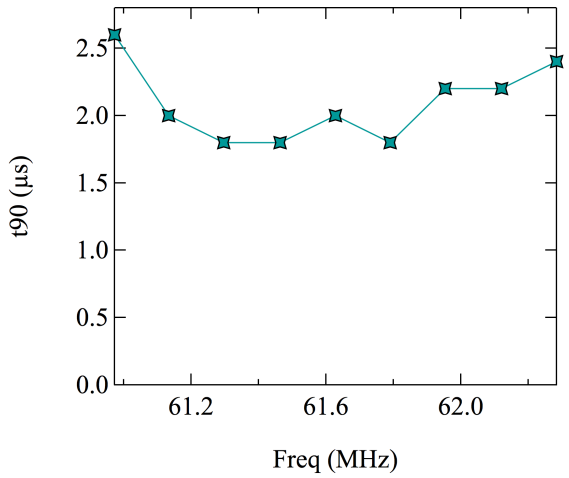

FIG. 13.— Values of t_{90} at each frequency corresponding to the nine peaks of the 0° spectrum.

3.4. t_{90} *Frequency Dependence Study*

We also investigated if t_{90} has frequency dependence, independent of angle. We nutated at each of the peak frequencies at 0° to find t_{90}. Figure 13 shows the dependence of t_{90} on frequency. t_{90} increases at the satellite peaks, with an overall range from 1.8μs to 2.6μs. A longer t_{90} at the satellites means that at these frequencies, the pulse length that we used was too short to rotate the magnetic moment 90°. This would contribute, along with the effect of T_2^{-1} frequency dependence, to the decreased intensity of the satellite peaks in our frequency sweeps. For the frequency sweeps in our angular dependent studies, the parameter t_{90} parameter was optimized at the central frequency at 0°. As a function of angle, the central frequency increased, therefore t_{90} may no longer have been optimized at larger angles.

4. FUTURE WORK

David Nisson has been working with comparing theoretical calculations for the nutations and frequency sweeps to the data outlined in this paper. Further analysis of this data could include fitting the evolution of peak frequencies as a function of angle, and calculating the carrier concentration in the sample from comparing data we took at 10K with calculations previously made by David Nisson. Further experimental work could be done looking at T_2^{-1} dependence with a finer spacing of data points and looking at the frequency dependence of T_1. This sample of Bi_2Se_3 could be further studied through NMR by examining the effects of altering parameters other than angle, such as temperature, external magnetic field, and pressure.

The properties of Bi_2Se_3 characteristic of topological insulators could potentially be studied through NMR on materials with a higher surface to area volume ratio, such as nanowires. If our theoretical models do not predict some of the results described in this paper, investigations could be made into whether they were the results of interactions with the surface states of the material.

5. CONCLUSIONS

In this study, we carefully examined the angular dependence of t_{90} and the resonant frequencies in the bismuth signal in a single crystal cut from our sample of Bi_2Se_3 through NMR. We also measured the dependence of T_2^{-1} and t_{90} on frequency at 0°. We were also able to locate the ^{77}Se signal in a larger powder sample.

Our examination of the NMR properties of Bi_2Se_3 as a function of angle in an external magnetic field assisted in characterizing the bulk of the material. This information is vital if bismuth selenide is to be potentially used in technology. Nuclear magnetic resonance can also aid in probing properties of the spin states of the electrons in the material, which is essential knowledge in the creation of spintronics devices.

I would like to thank my advisor Nicholas Curro, as well as Adam Dioguardi, Peter Klavins, David Nisson, John Crocker, Jim Lin, and all the other members of the UC Davis physics NMR Lab. I would like to thank Rena Zieve for organizing the REU program and I would like to acknowledge NSF grant PHY-1263201 for funding my research. I would also like to thank Kirill Kovnir in the UC Davis chemistry department for allowing us to use his x-ray diffraction machine, and grad student Katherine Woo for assisting us in taking our XRD measurement.

REFERENCES

[1]Adam Dioguardi, *Nuclear Magnetic Resonance Studies of the 122 Iron-Based Superconductors*, University of Davis, Davis, California, 2013.

[2]M. Z. Hasan and C. L. Kane, Colloquium: Topological insulators, *Rev. Mod. Phys*, 82, 3045, 2010.

[3]D. M. Nisson, A. P. Dioguardi, X. Peng, D. Yu, and N. J. Curro, *Anomalous nuclear magnetic resonance spectra in Bi2Se3 nanowires*, University of Davis, Davis, California, 2014.

[4]C. P. Slichter, Principles of Magnetic Resonance (Springer Series in Solid-State Sciences), Springer-Verlar, 1990.

[5]R. E. Taylor, B. Leung, M. P. Lake, and L.-S. Bouchard, Spin-Lattice Relaxation in Bismuth Chalcogenides, *J. Phys. Chem. C*, 116, 17300-17305, 2012.

[6]B. Young, Z. Lai, Z. Xu, A. Yang, G. D. Gu, Z.-H. Pan, T. Valla, G. J. Shu, R. Sankar, and F. C. Chou, Probing the bulk electronic states of Bi2Se3 using nuclear magnetic resonance, *Phys. Rev.*, B 86, 075137, 2012.

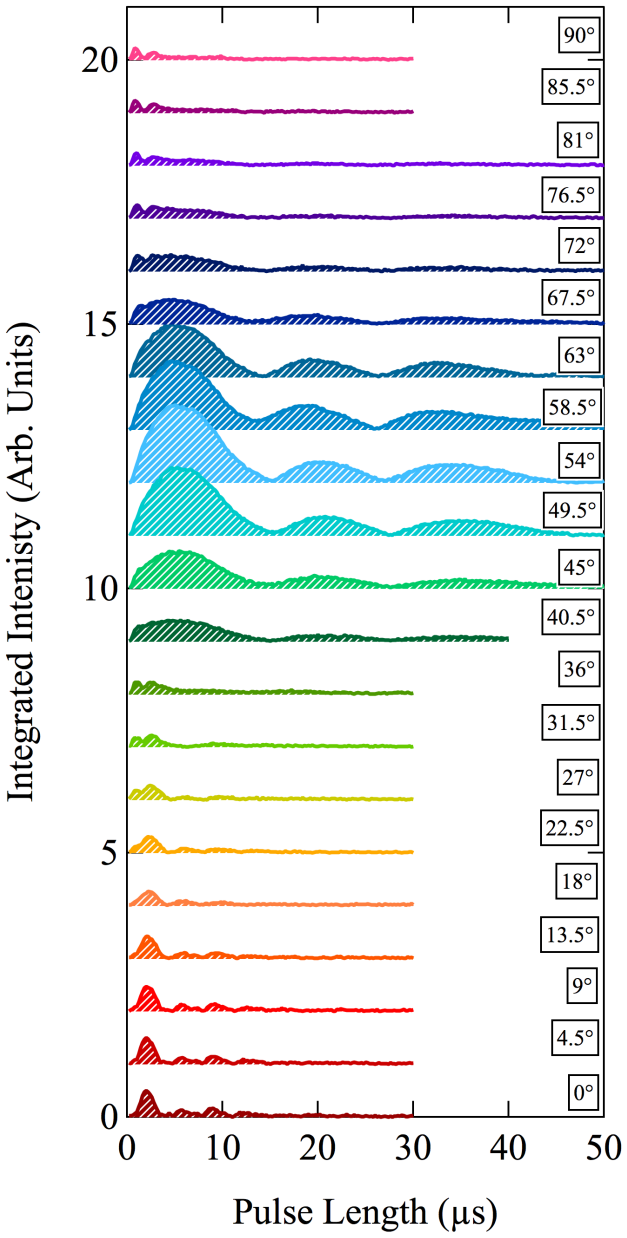

FIG. 14.— Nutations of Bi_2Se_3 crystal sample as a function of angle in the external magnetic field from 0° to 90°.

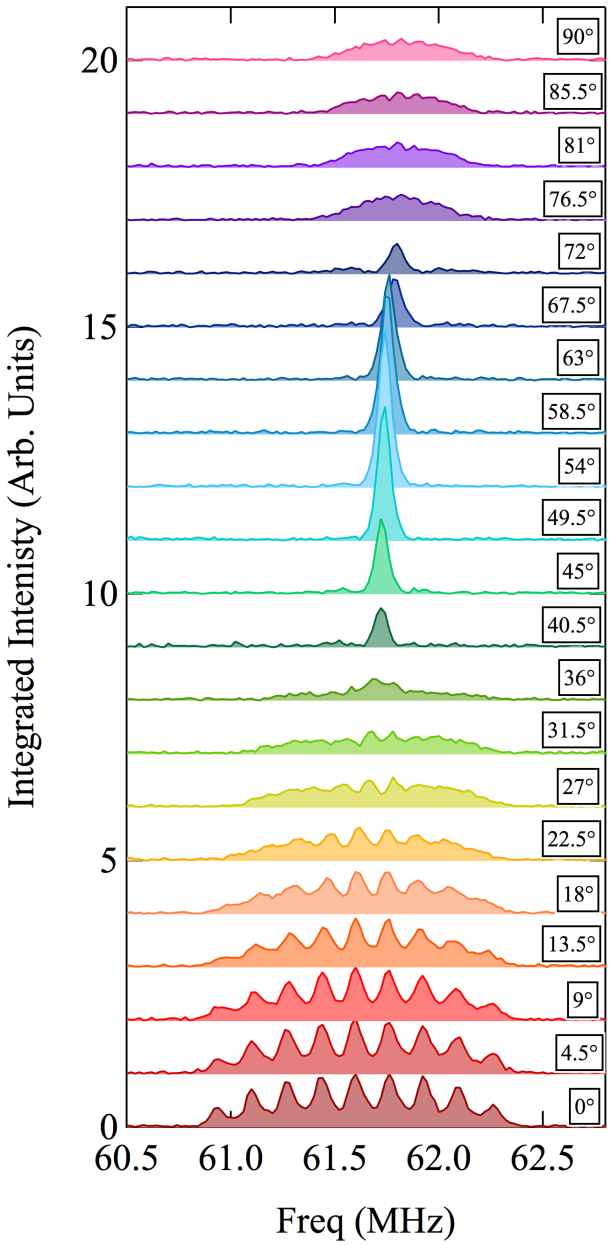

FIG. 15.— Frequency sweeps of Bi_2Se_3 crystal sample as a function of angle in the external magnetic field from 0° to 90°.